



# Atomic force microscopy based repeatable surface nanomachining for nanochannels on silicon substrates

Zhuxin Dong<sup>\*,1</sup>, Uchechukwu C. Wejinya<sup>2</sup>

Department of Mechanical Engineering, University of Arkansas, Fayetteville, AR 72701, USA

## ARTICLE INFO

### Article history:

Received 5 December 2011  
Received in revised form 23 April 2012  
Accepted 15 May 2012  
Available online 29 May 2012

AFM  
Surface nanomachining  
Diamond tip  
Si substrate  
Linear and logarithmic fit

## ABSTRACT

The atomic force microscopy (AFM)-based repeatable nanomachining for nanochannels on bare silicon surfaces is investigated experimentally for automated nano manufacturing applications. The relationship between the normal force applied on the AFM cantilever and the channel depth is established and analyzed using both linear and logarithmic fits. Thus, current results can be regarded as the calibration reference in order to accurately predict the nanochannel depth for additional nanotechnology related applications. An accurate prediction of the depth is not only for accuracy and efficiency, but also to prevent a costly diamond tip from unnecessary wear and tear. Furthermore, the experimental results also reveal that the fabrication procedure is repeatable.

© 2012 Elsevier B.V. All rights reserved.

## 1. Introduction

Among current nanotechnology applications, the design and fabrication of nanochannels are one of the major challenges. To date, the methods for fabricating nanochannels have included bulk nanomachining and wafer-bonding [1,2], surface nanomachining [3], buried channel technology [4] and nanoimprint lithography [5–7]. Nanochannels that are 50 nm deep and 5  $\mu\text{m}$  wide [1,2], 20–100 nm deep and 0.5–20  $\mu\text{m}$  wide [3], and 10 nm deep and 50 nm wide [5] have been demonstrated. Although nanoimprint lithography can fabricate 2-dimensional nanochannels [6,7], these channels are all fabricated by complex processing methods that require sophisticated masking and etching. Thus, a means by which nanochannels are able to be fabricated without complex processing and reach to nano level in 3-dimension becomes necessary.

Since atomic force microscopy (AFM) was invented in 1986 [8], it has been widely used in fields of material science, biomedicine, and nanofabrication. AFM-based nanolithography [9] offers a simple and reliable technique for mechanically machining nanochannels on substrates such as polymer [10–12], metal [13], semiconductor [14–16], and insulator [17]. However, nanochannels on a bare silicon substrate produced by AFM-based nanolithography with a diamond tip have not been reported yet. In this paper, a study of the nanochannels on bare silicon surfaces fabricated by AFM-based

nanoscratching is reported and experimental results show that this technique can be applied in the fabrication of carbon nanotube (CNT)-ion sensitive field effect transistor (ISFET) based structure, where relatively large nanochannels on the silicon substrate are needed for the deposition and alignment of bundles of CNTs [18].

## 2. Experimental setup

The experiment is performed using an Agilent 5500 AFM (Agilent Technologies Inc., Santa Clara, CA, USA) with the Head Electronics Box that provides an oscillating voltage for AC (tapping) mode imaging as shown in Fig. 1. A hand-crafted high force cantilever with a diamond tip for nanoindentation/nanoscratching is used to produce the nanochannels (DNISP, Bruker Corporation). The cantilever is pre-calibrated with a normal spring constant ( $K_C$ ) of 244 N/m. The radius of the diamond tip is 40 nm. The diamond tip apex is similar to the corner of cube so that three right angle planes form an “A”-shape apex. This is used for all nanolithography-related operations. The cantilever is made of stainless steel with a normal elastic modulus ( $E$ ) of 193 GPa and a shear modulus ( $G$ ) of 80 GPa. The sensitivity ( $S_Z$ ) of position-sensitive-detector (PSD) is 255 nm/V.

Fig. 2 illustrates the schematic of the experimental setup for creating nanochannels on a polished silicon layer (625  $\mu\text{m}$  thick). The topographies are scanned under AC mode, while scratching is completed under Contact mode where the vertical deflection of the cantilever is kept constant and controlled by the setpoint ( $S_T$  in

\* Corresponding author. Tel.: +1 479 575 4800; fax: +1 479 575 6982.  
E-mail address: [dzhuxin@uark.edu](mailto:dzhuxin@uark.edu) (Z. Dong).

<sup>1</sup> Student Member, IEEE.

<sup>2</sup> Member, IEEE.

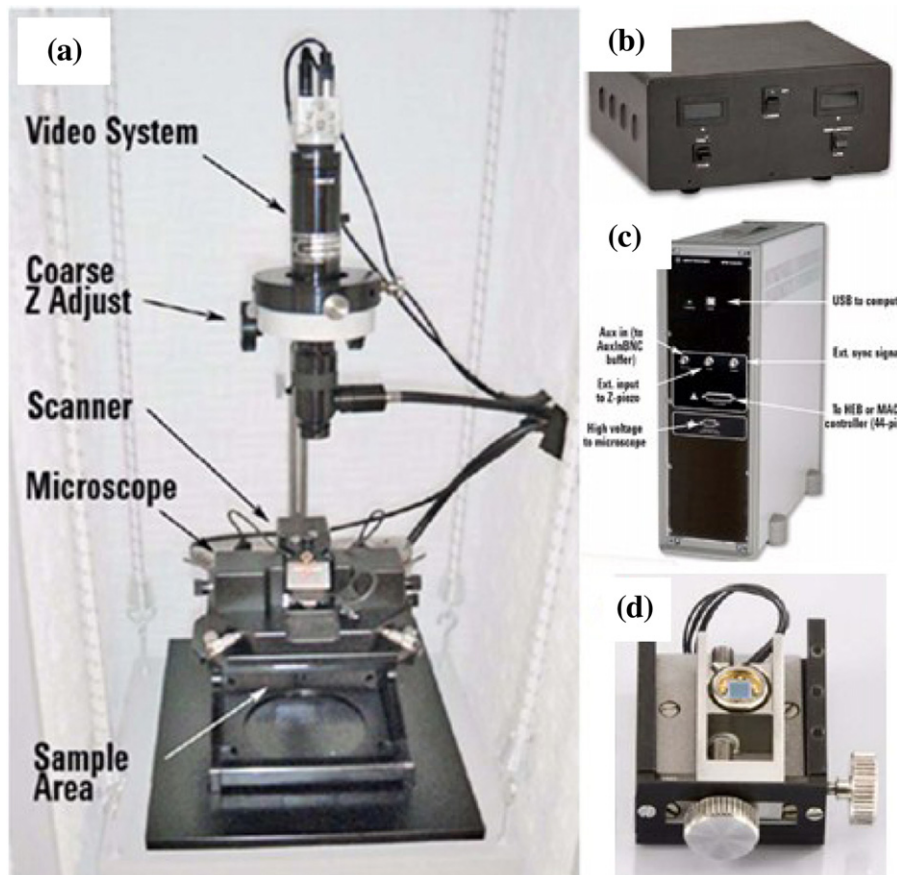


Fig. 1. Experimental setup for AFM-based nanolithography: (a) the microscope; (b) head electronics box; (c) AFM controller; and (d) PSD bottom-view.

V). Therefore, once the setpoint is specified, the scratching normal force ( $F_N$ ) can be computed as follows Eq. (1) [19]:

$$F_N = K_C \times S_Z \times S_T \quad (1)$$

### 3. Experimental results

#### 3.1. Scratching velocity effect

Before scratching on samples, three user-controllable parameters that may affect the dimensions of the nanochannels need to be determined. These parameters are the scratching velocity, the

scratching normal force (the setpoint) and the number of times that the tip scratches. Through the single nanomachining experiment, it was observed that the variation of scratching velocity is negligible for predicting the dimensions. Fig. 3 presents 25, 5- $\mu\text{m}$ -long nanochannels that are fabricated by single-scratch, but with different  $F_N$  from (a) to (e), at different scratching velocities from I to V. Take Fig. 3(a) for example: it has five channels, all of which are fabricated under  $F_N = 31.11 \mu\text{N}$ , but the scratching velocity varies from 0.1  $\mu\text{m/s}$ , 0.25  $\mu\text{m/s}$ , 0.5  $\mu\text{m/s}$ , 0.75  $\mu\text{m/s}$  and 1  $\mu\text{m/s}$  for nanochannel I, II, III, IV, and V, respectively. No trends about significant dimensional changes were observed either from the vision of figure or the measurement of nanochannel depth and width as the scratching velocity increases.

In Fig. 3, nanochannels in part (a), (b), (c), (d), and (e) were fabricated in different locations. However, every five nanochannels (I, II, III, IV, and V) in each part were fabricated continuously. Take part (a) for instance as shown in Fig. 4, the AFM tip started scratching at Point 1 with a normal force of 31.11  $\mu\text{N}$  until it reached Point 2. After this process, the normal force should return to an original value when it moved from Point 2 to 3. This normal force was caused by the setpoint used when switched from AC mode to Contact mode during imaging, and it has to be positive in order to maintain the contact between the tip and the sample. During scratching from Point 3 to 4, a normal force of 62.22  $\mu\text{N}$  was applied. After repeating the scratching procedure, i.e., 1–2, 3–4, 5–6, 7–8, 9–10 and moving from 2–3, 4–5, 6–7, 8–9, 10–1, the tip moved back to the origin position of Point 1 by system default. Due to the setpoint in Contact mode, there were diagonals left when the tip moved from an end point to a start point. We also measured and analyzed these diagonals and found they were much smaller than the nanochannels next to them. In addition, the reason why there was a lot of

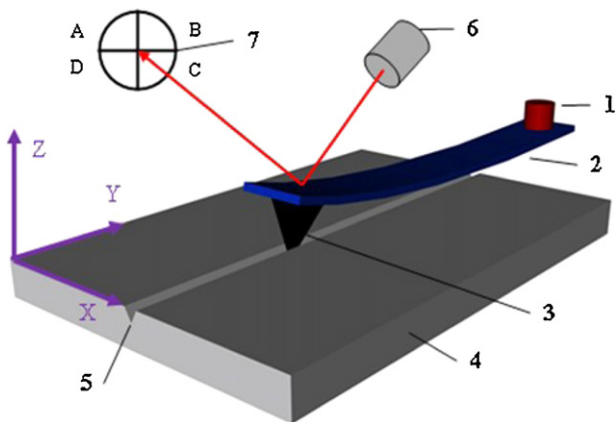


Fig. 2. Schematics of nanoscratching: (1) piezo scanner for XYZ movement; (2) cantilever; (3) diamond tip; (4) silicon; (5) nanochannel; (6) laser; and (7) four-quadrant PSD.

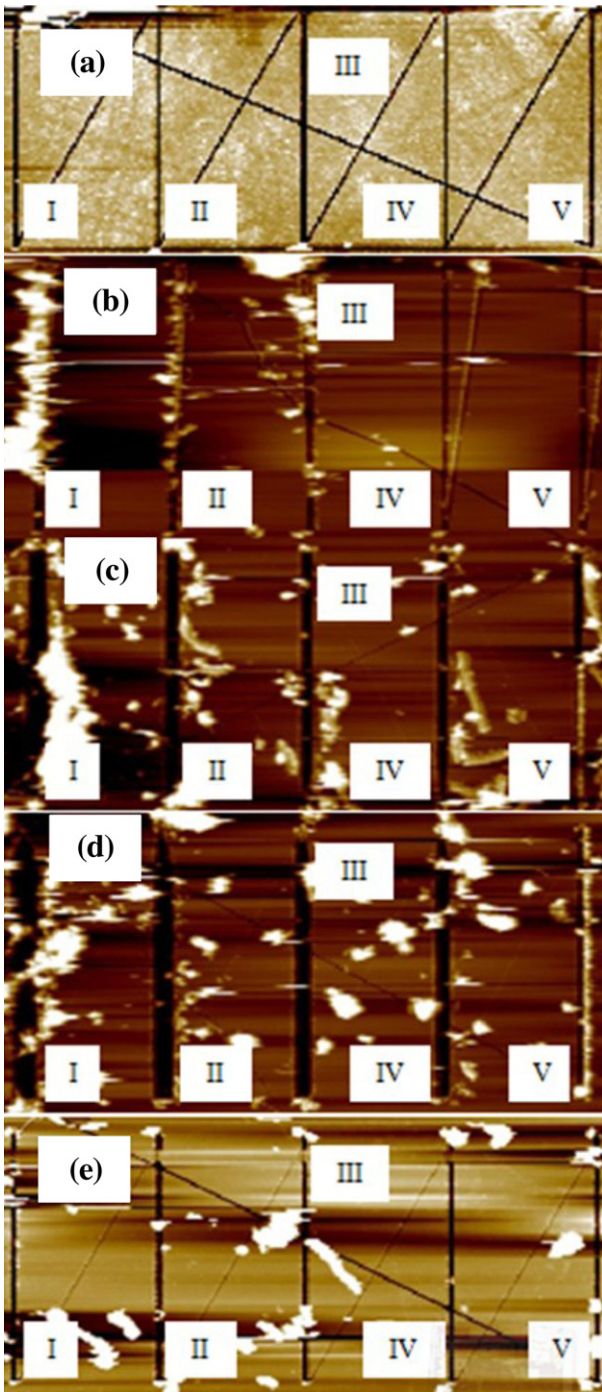


Fig. 3. AFM topographies of nanochannels (5  $\mu\text{m}$ ) scratched at different normal forces ( $\mu\text{N}$ ) of (a) 31.11, (b) 62.22, (c) 93.33, (d) 124.44 and (e) 155.55, and scratching velocities ( $\mu\text{m/s}$ ) of (I) 0.1, (II) 0.25, (III) 0.5, (IV) 0.75 and V 1.

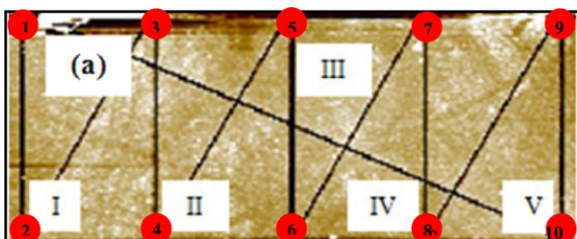


Fig. 4. Route for continuous fabrication of five nanochannels at different settings.

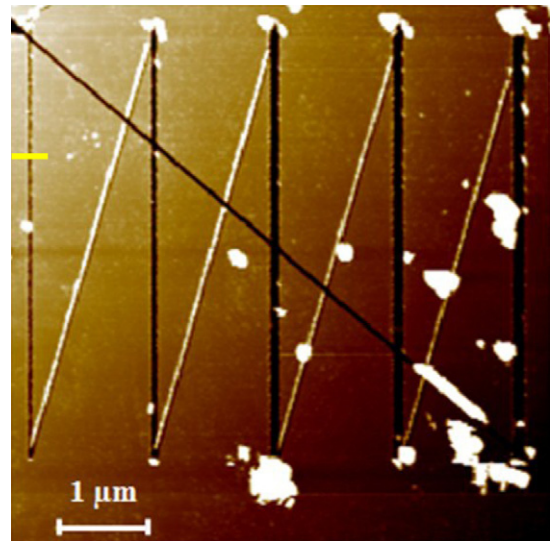


Fig. 5. Topography of single-scratching test at a constant velocity (0.1  $\mu\text{m/s}$ ): 5- $\mu\text{m}$ -long channels scratched from left to right at normal forces ( $\mu\text{N}$ ) of 31.11, 62.22, 93.33, 124.44 and 155.55, respectively.

scratching residuals in the topographies was that five deep nanochannels were fabricated in  $7 \mu\text{m} \times 7 \mu\text{m}$  tiny area and imaged immediately after the fabrication. The issues were only caused by automatically fabricating multiple nanochannels at a time. In future application, we can fabricate single nanochannel at a time, so these issues will no longer exist. Furthermore, if multiple channels need to be fabricated simultaneously in certain application, the setpoint can be set as low as 0.1 V which will maintain the contact and negligible diagonal depths.

### 3.2. Scratching normal force effect

In order to investigate the relationship between the dimension of nanochannels and the scratching normal force, single surface nanomachining is implemented. In this test, the scratching velocity is kept constant at 0.1  $\mu\text{m/s}$ , and five 5- $\mu\text{m}$ -long nanochannels are fabricated at different normal forces of 31.11  $\mu\text{N}$ , 62.22  $\mu\text{N}$ , 93.33  $\mu\text{N}$ , 124.44  $\mu\text{N}$  and 155.55  $\mu\text{N}$ . Then, five measurements for each nanochannel are recorded as shown in Table 1. Fig. 5 presents the topography for the nanochannels. Furthermore, Fig. 6 shows how to take the dimensional measurement by drawing arbitrary cross-section line over target. Finally, the linear relationship between the depth of nanochannels and the scratching normal force for single surface nanomachining is obtained as shown in Fig. 7.

### 3.3. Repeatable scratching effect

Furthermore, the relationship between the depth of nanochannel and the normal force in double surface machining is also studied. The scratching velocity was kept at 0.1  $\mu\text{m/s}$ , but the

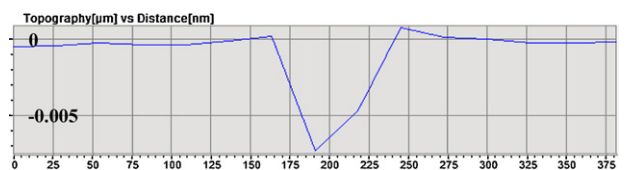


Fig. 6. Illustration of nanochannel dimensional measurement: give the Z-axis information of the yellow cross-section line in Fig. 5. (For interpretation of the references to color in this figure legend, the reader is referred to the web version of the article.)

**Table 1**  
Depth measurement for single surface nanomachining.

Channel (left to right)	Force ( $\mu\text{N}$ )	Depth (nm)					Mean (nm)	St. Dev. (nm)
1	31.11	5.32	4.55	7.90	6.42	6.29	6.09	1.26
2	62.22	16.2	17.4	18.2	18.8	15.3	17.2	1.42
3	93.33	28.0	22.3	25.3	23.0	25.8	24.9	2.28
4	124.44	30.3	28.0	33.5	29.5	31.8	30.6	2.11
5	155.55	32.3	35.0	35.5	36.7	40.7	36.1	3.04

**Table 2**  
Depth measurement for double surface nanomachining.

Channel (left to right)	Force ( $\mu\text{N}$ )	Depth (nm)					Mean (nm)	St. Dev. (nm)
1	31.11	7.55	16.5	10.3	13.9	14.6	12.6	3.60
2	62.22	35.7	32.4	35.0	37.4	34.3	35.0	1.82
3	93.33	49.0	45.2	48.7	44.9	36.3	44.8	5.12
4	124.44	136	141	91.0	130	148	129	22.4
5	155.55	107	113	101	92.2	106	104	7.67

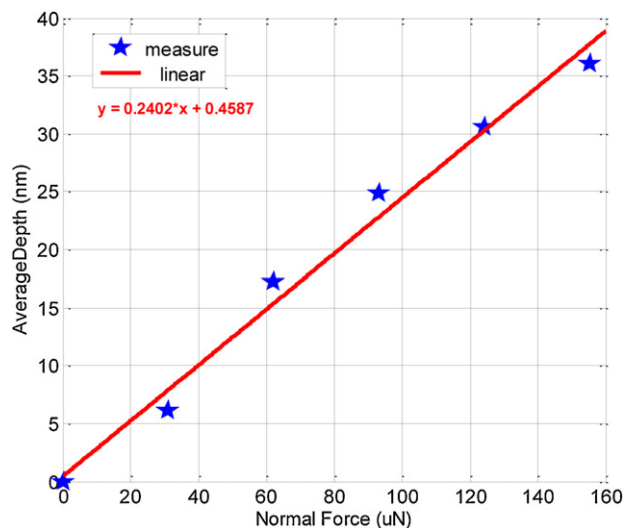


**Fig. 7.** Relationship between depth and force for single-scratching. Linear fit slope and  $R^2$  value are 0.2402 nm/ $\mu\text{N}$  and 0.9859, respectively.

surface will be scratched twice by the diamond tip to fabricate each 5- $\mu\text{m}$ -long channel at different normal forces of 31.11  $\mu\text{N}$ , 62.22  $\mu\text{N}$ , 93.33  $\mu\text{N}$ , 124.44  $\mu\text{N}$  and 155.55  $\mu\text{N}$ . Fig. 8 shows the topography of the channels, and their depth information is recorded in Table 2. Furthermore, the linear relationship between the depth of nanochannels and the scratching normal force for double surface nanomachining is shown in Fig. 9.

#### 3.4. Logarithmic correlation

As discussed previously, we assume the linear correlations between the nanochannel dimension and the normal force start at the origin (0, 0), which means a nanochannel appears no matter how small the normal force is. This assumption may not be completely precise. A more reasonable prospect is that a threshold of the normal force exists. No nanochannel can be fabricated unless the normal force exceeds this threshold, and this threshold should depend on material properties of both the surface and the AFM tip. However, the linear correlation cannot present the meaning in this level. In contrary, the linear correlation may mislead us to some confusion. Take Fig. 6 for example, according to the linear correlation, a 0.4587-nanometer-deep channel will be fabricated with a normal force of zero magnitude which theoretically and physically cannot be true (a 0.9632-nanometer-deep channel would appear and the slope becomes 0.2357 according to the linear correlation

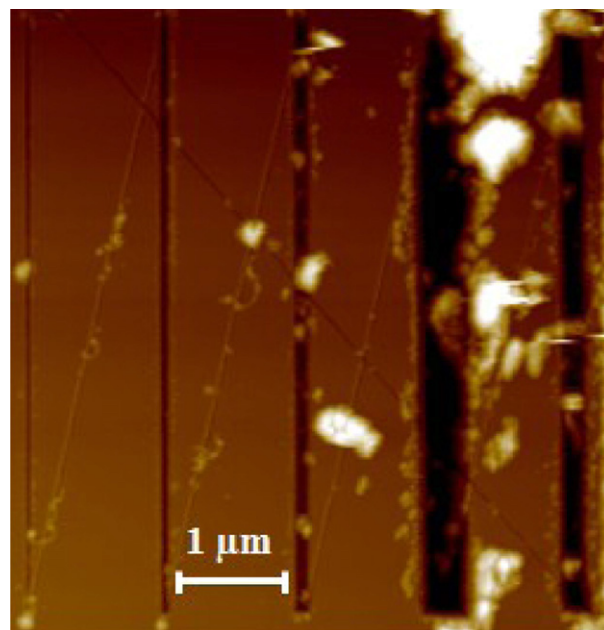


**Fig. 8.** Double-scratching test at a constant velocity (0.1  $\mu\text{m/s}$ ): 5- $\mu\text{m}$ -long channels scratched from left to right at normal forces ( $\mu\text{N}$ ) of 31.11, 62.22, 93.33, 124.44 and 155.55, respectively.

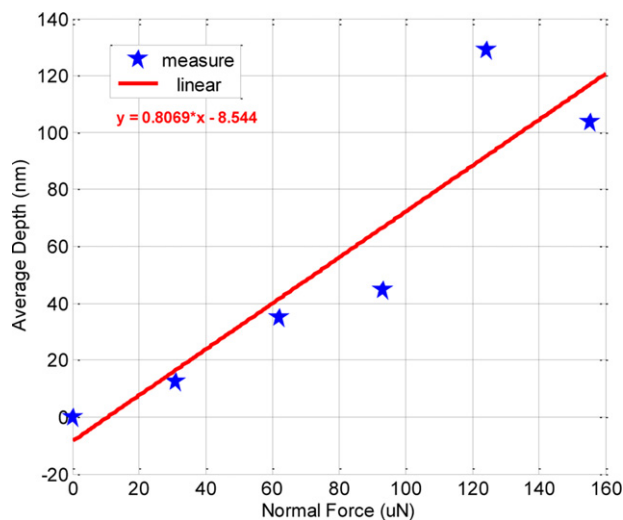


**Fig. 9.** Relationship between depth and force for double-scratching. Linear fit slope and  $R^2$  value are 0.8069 nm/ $\mu\text{N}$  and 0.8352, respectively.

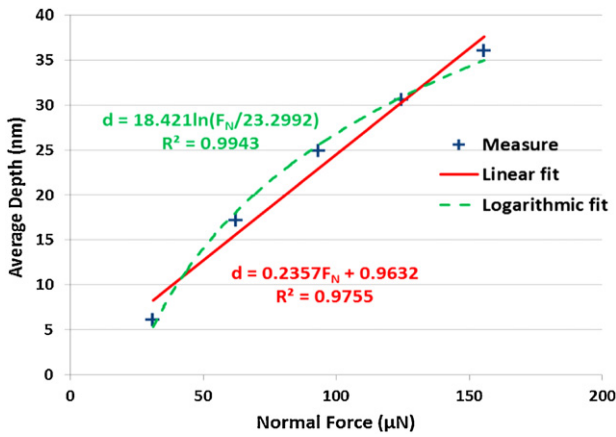


Fig. 10. Comparison of linear and logarithmic correlations between channel depth and applied normal force for single scratching.

obtained without the origin point). In addition, logarithmic correlations do possess a better coefficient of determination ( $R^2$  value) [20,21]. Therefore, the logarithmic correlation as shown in Eqs. (2) and (3) is employed to represent the results on nanochannel depth and width, respectively.

$$d = \alpha_1 \ln \left( \frac{F_N}{F_{t1}} \right) \quad (2)$$

$$w = \alpha_2 \ln \left( \frac{F_N}{F_{t2}} \right) \quad (3)$$

where  $\alpha_1$  and  $\alpha_2$  are the scratching penetration depth and penetration width, respectively, and  $F_{t1}$  and  $F_{t2}$  are the threshold forces depending on the depth and width data, respectively.

Fig. 10 shows both the linear and logarithmic correlations between the nanochannel depth and the normal force for single scratching. Hence, the scratching penetration depth is 18.421 nm, and the threshold force is 23.2992  $\mu\text{N}$ . The logarithmic method possesses a better coefficient of determination ( $R^2$ ) as expected. The same approach is used for the width as shown in Fig. 11, where the logarithmic method also has a better performance and the penetration width and the threshold force are 54.605 nm and 7.41889  $\mu\text{N}$ , respectively. Figs. 12 and 13 illustrate the comparison between the linear and logarithmic correlations for repeated scratching, where neither of the two correlations possesses a good  $R^2$  value. The main issue may lie in the experimental data collected from repeated scratching as the fourth channel (from left to right) in Fig. 7 is fabricated beyond expected. It brings an unexpected large point in the data series. The new results and data show that our experimental

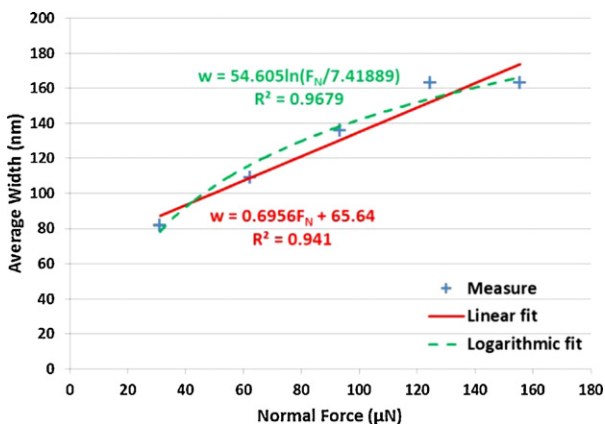


Fig. 11. Comparison of linear and logarithmic correlations between channel width and applied normal force for single scratching.

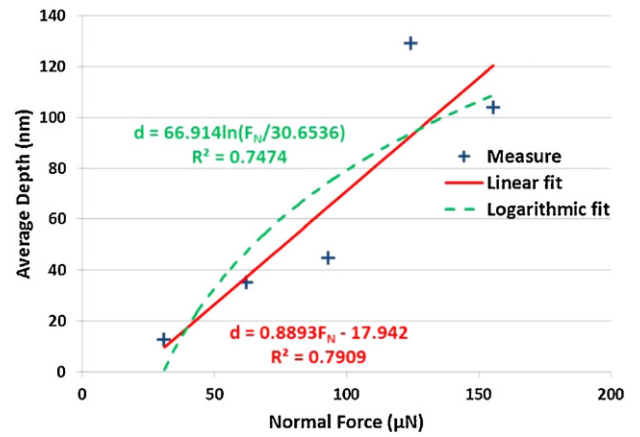


Fig. 12. Comparison of linear and logarithmic correlations between channel depth and applied normal force for repeated scratching.

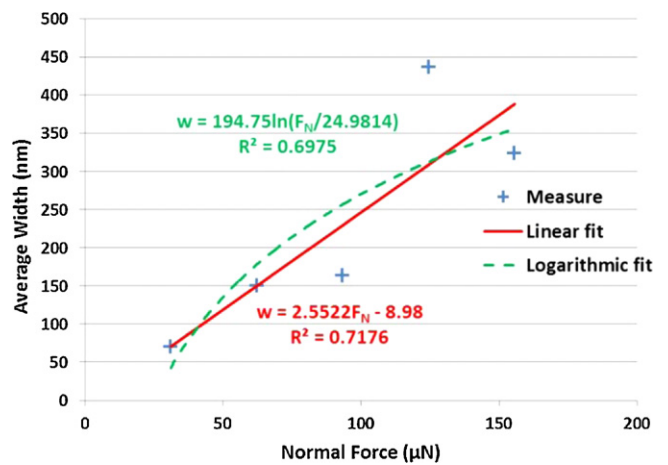


Fig. 13. Comparison of linear and logarithmic correlations between channel width and applied normal force for repeated scratching.

setup is correct and repeatable. The depth and width of the channel created with normal force of 124.44  $\mu\text{N}$  are experimentally verified that they should be within the values of normal force of 93.33  $\mu\text{N}$  and 155.55  $\mu\text{N}$ . Also, the linear correlation possesses a higher coefficient of determination in repeatable scratching. Figs. 14 and 15 are one of the extra experimental results to illustrate the correlations between the channel dimensions and different normal forces with a constant scratching number of 2.

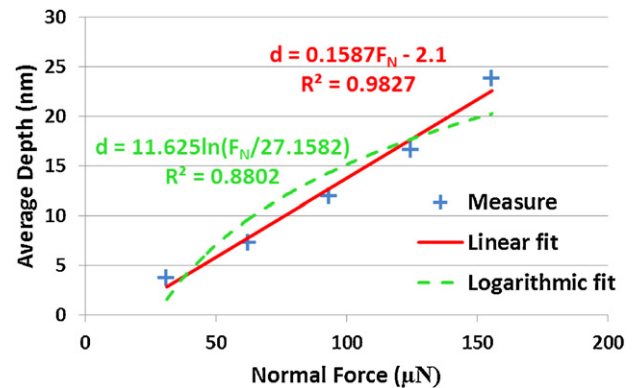


Fig. 14. Additional linear and logarithmic correlations between channel depth and applied normal force for repeated scratching.

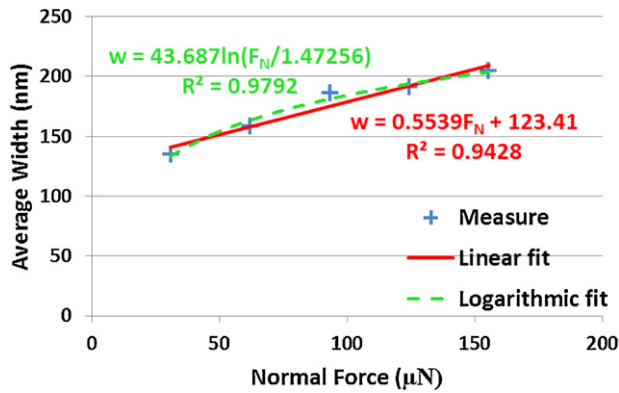


Fig. 15. Additional linear and logarithmic correlations between channel width and applied normal force for repeated scratching.

### 3.5. Variation of scratching number

An experiment was conducted to conclude on the dimensional changes caused by an increasing scratching number. Fig. 16(a) shows five 3- $\mu\text{m}$ -long nanochannels. Fig. 16(b) and (c) are the height profiles. They were fabricated at constant speed (0.1  $\mu\text{m}/\text{s}$ ) and normal force (31.11  $\mu\text{N}$ ) but with different scratching numbers from 1 to 5. Their mean depths were 0.837, 1.71, 2.45, 2.79 and 2.99 nm respectively, and the corresponding standard deviations were 0.141, 1.195, 0.141, 0.188, and 0.152 nm respec-

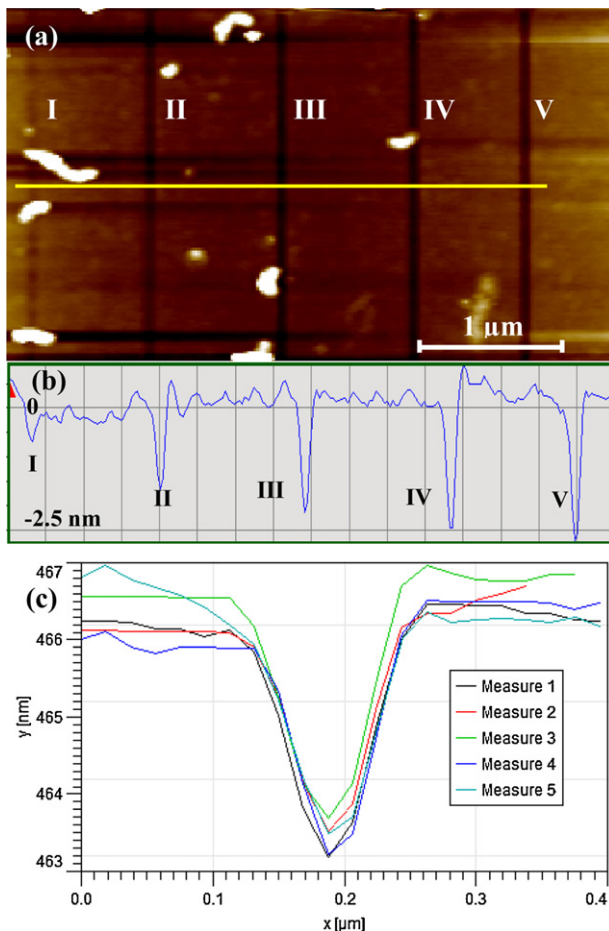


Fig. 16. Test of varying scratching number, channel I–V corresponding to scratching number 1–5: (a) topography, (b) corresponding height profile of the cross section line, and (c) the height profile of channel V including 5 measurements.

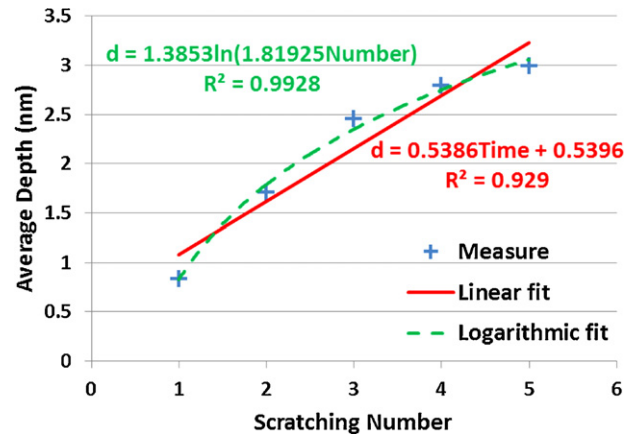


Fig. 17. Comparison of linear and logarithmic correlations between channel depth and scratching numbers at constant normal force of 31.11  $\mu\text{N}$ .

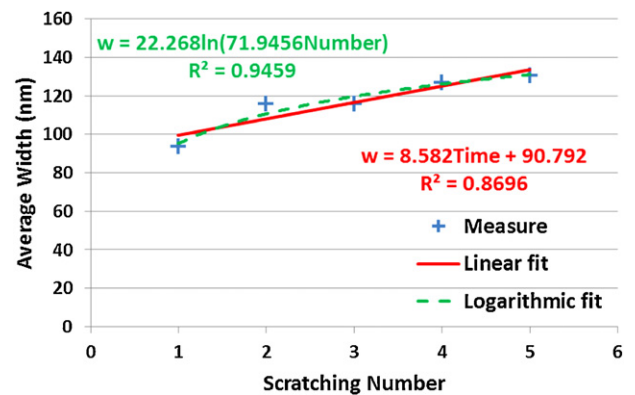


Fig. 18. Comparison of linear and logarithmic correlations between channel width and scratching numbers at constant normal force of 31.11  $\mu\text{N}$ .

tively. Although these five channels were still close to each other spacing wise, they were scratched separately. Therefore, the diagonals no longer exist. As shown in Figs. 17 and 18, deeper and wider channels were fabricated as the scratching number was increased as expected. Additionally, the logarithmic correlation possessed higher coefficient of determination especially for the depth. Furthermore, it was observed that it is more logarithmic when scratching nanochannels at a constant normal force with increasing scratching number while it is more linear when scratching twice with increasing normal force.

## 4. Conclusion

This paper proposes an AFM-based repeatable surface nanomachining for fabricating nanochannels on bare silicon substrate, which is simple and effective. A hand-crafted high force cantilever with a diamond tip for nanoindenting/nanoscratching is involved. Nanochannels are fabricated to study the relationship between the channel depth and various combinations of parameter setting. Based on the current results, we find that the normal force and the scratching number are the key factors which dominate the fabrication performance but the scratching velocity is negligible. However, when we increase either the normal force or the scratching number, the channel dimensions increase differently. The comparison between the linear and logarithmic correlations of the dimensions of nanochannels and the applied normal force is given and analyzed. These correlations are of great value for accurately predicting the scratching performance when the nanochannels are fabricated using such a system. The experimental results can be regarded

as a reference in order to increase the efficiency in nanochannel fabrication and prevent the costly diamond tip from unnecessary wear and tear in the future when nanochannels with depth range between 5 nm to 100 nm are needed on Si surface. In addition, the nanochannel fabrication time for these automated experiments was determined to be less than 3 min for channel length of 5  $\mu\text{m}$  for 5 different channels or 50 s for a single channel. The time could be reduced further if the channel length is decreased and the fabrication speed is increased.

## References

- [1] J. Haneveld, H. Jansen, E. Berenschot, N. Tas, M. Elwenspoek, Wet anisotropic etching for fluidic 1D nanochannels, *Journal of Micromechanics and Microengineering* 13 (2003) S62–S66.
- [2] A. Datta, S. Gangopadhyay, H. Temkin, Q. Pu, S. Liu, Nanofluidic channels by anodic bonding of amorphous silicon to glass to study ion-accumulation and ion-depletion effect, *Talanta* 68 (2006) 659–665.
- [3] M.B. Stern, M.W. Geis, J.E. Curtin, Nanochannel fabrication for chemical sensors, *Journal of Vacuum Science and Technology B* 15 (6) (1997) 2887–2891.
- [4] M.J. de Boer, R.W. Tjerkstra, J.W. Berenschot, H.V. Jansen, C.J. Burger, J.G.E. Gardeniens, M. Elwenspoek, A. van den Berg, Micromachining of buried micro channels in silicon, *Journal of Microelectromechanical Systems* 9 (2000) 94–103.
- [5] H. Cao, J.O. Tegenfeldt, R.H. Austin, S.Y. Chou, Gradient nanostructures for interfacing microfluidics and nanofluidics, *Applied Physics Letters* 81 (16) (2002) 174–176.
- [6] L.J. Guo, X. Cheng, C.F. Chou, Fabrication of size-controllable nanofluidic channels by nanoimprinting and its application for DNA stretching, *Nano Letters* 4 (1) (2004) 69–73.
- [7] J.O. Tegenfeldt, C. Prinz, H. Cao, R.L. Huang, R.H. Austin, S.Y. Chou, E.C. Cox, J.C. Sturm, Micro- and nanofluidics for DNA analysis, *Analytical and Bioanalytical Chemistry* 378 (7) (2004) 1678–1692.
- [8] G. Binnig, C.F. Quate, Ch. Gerber, Atomic force microscope, *Physical Review Letters* 56 (March) (1986) 930–933.
- [9] X.N. Xie, H.J. Chung, C.H. Sow, A.T.S. Wee, Nanoscale materials patterning and engineering by atomic force microscopy nanolithography, *Materials Science and Engineering R: Reports* 54 (November (1–2)) (2006) 1–48.
- [10] J.-M. Chen, S.-W. Liao, Y.-C. Tsai, Electrochemical synthesis of polypyrrole within PMMA nanochannels produced by AFM mechanical lithography, *Synthetic Metals* 155 (1) (2005) 11–17.
- [11] B. Cappella, H. Sturm, Comparison between dynamic plowing lithography and nanoindentation methods, *Journal of Applied Physics* 91 (2002) 506–512.
- [12] M. Heyde, K. Rademann, B. Cappella, M. Geuss, H. Sturm, T. Spangenberg, H. Niehus, Dynamic plowing nanolithography on polymethylmethacrylate using an atomic force microscope, *Review of Scientific Instruments* 72 (2001) 136–141.
- [13] Z. Kato, M. Sakairi, H. Takahashi, Nanopatterning on aluminum surfaces with AFM probe, *Surface and Coatings Technology* 169–170 (2003) 195–198.
- [14] J.C. Rosa, M. Wendel, H. Lorenz, J.P. Kotthaus, Direct patterning of surface quantum wells with an atomic force microscope, *Applied Physics Letters* 73 (18) (1998) 2684–2686.
- [15] J. Regul, U.F. Keyser, M. Paesler, F. Hohls, U. Zeitler, R.J. Haug, A. Malave, E. Oesterschulze, D. Reuter, A.D. Wieck, Fabrication of quantum point contacts by engraving GaAs/AlGaAs heterostructures with a diamond tip, *Applied Physics Letters* 81 (2002) 2023–2025.
- [16] P.A. Fontaine, E. Dubois, D. Stievenard, Characterization of scanning tunneling microscopy and atomic force microscopy-based techniques for nanolithography on hydrogen-passivated silicon, *Journal of Applied Physics* 84 (August (4)) (1998) 1776–1881.
- [17] Z.Q. Wang, N.D. Jiao, S. Tung, Z.L. Dong, Atomic force microscopy-based repeated machining theory for nanochannels on silicon oxide surfaces, *Applied Surface Science* 257 (2011) 3627–3631.
- [18] Z. Dong, U.C. Wejinya, S.N.S. Chalamalasetty, M.R. Margis, Atomic force microscopy based nano manipulation towards CNT-ISFET pH sensing system, in: *Proceedings of the IEEE 6th International Conference on Nano/Micro Engineered and Molecular Systems (NEMS 2011)*, Kaohsiung, Taiwan, February 20–23, 2011.
- [19] B. Bhushan, *Nanotribology and Nanomechanics*, Springer-Verlag, Berlin, Heidelberg, 2008.
- [20] A.A. Tseng, J.-i. Shirakashi, S. Nishimura, K. Miyashita, A. Notargiacomo, Scratching properties of nickel–iron thin film and silicon using atomic force microscopy, *Journal of Applied Physics* 106 (2009) 044314.
- [21] A.A. Tseng, A comparison study of scratch and wear properties using atomic force microscopy, *Applied Surface Science* 256 (2010) 4246–4252.

**Zhuxin Dong** (S'07) received his B.E. degree in Biomedical Engineering from Shenyang University of Technology in 2005. Also in the same year, he was admitted by The Chinese University of Hong Kong (CUHK) and joined Centre for Micro and Nano Systems (CMNS). He worked as a member of the 3D Digital Pen Team in CMNS and obtained his M. Phil. degree in Mechanical and Automation Engineering in 2007. Now, he is pursuing his Ph.D. degree in Department of Mechanical Engineering, University of Arkansas, US. His research interest covers calibration and application of MEMS-based  $\mu\text{IMU}$  for human motion sensing and recognition, application of Carbon Nanotube (CNT) based Nano devices, characterization and application of vertically-aligned carbon nanofibers (VACNFs), AFM-based nanoindentation and nanomanipulation, and Bio-MEMS.

**Uchechukwu C. Wejinya** (S'99–M'07) received his B.S. and M.S. degrees in Electrical and Computer Engineering from Michigan State University, East Lansing, MI, USA in 2000 and 2002, respectively. Upon completing his M.S. degree in 2002, he worked for General Motors research and development center where he conducted research on Magneto-Rheological Fluid (MRF) clutch system before returning to graduate school. He received a Ph.D. in electrical engineering in August 2007 from Michigan State University. After completing his Ph.D., he held a post-doctoral research position in the department of electrical and computer engineering at Michigan State University. In February 2008, he joined the department of mechanical engineering at the University of Arkansas where he holds the rank of assistant professor. His research interests include mechatronics with emphasis on nanotechnology–nanosensors including biosensors, chemical, nanoelectronics; control system design and application, electronics, micro-tools for handling and manufacturing of micro and nano devices, and modeling and simulation of micro and nano structures. He is the author and co-author of numerous conference and journal articles, and has presented at several national and international conferences. He was among the first group of USA graduate students to participate in the National Science Foundation, East Asia Pacific Summer Institute in Beijing, China in 2004 where he conducted research at the Chinese Academy of Sciences, Institute of Automation. In 2010, Dr. Wejinya received the Chinese Academy of Sciences Fellowship for Young International Scientist Award. Dr. Wejinya is a member of IEEE, ASME, NSBE, and ASEE.